



Kent Academic Repository

Strange, Paul (2018) *Quantized Hamiltonian Curl Forces and Squeezed Light*. Journal of Physics A: Mathematical and Theoretical, 51 (335303). ISSN 1751-8113.

Downloaded from

<https://kar.kent.ac.uk/68446/> The University of Kent's Academic Repository KAR

The version of record is available from

<https://doi.org/10.1088/1751-8121/aacecb>

This document version

Author's Accepted Manuscript

DOI for this version

Licence for this version

UNSPECIFIED

Additional information

Versions of research works

Versions of Record

If this version is the version of record, it is the same as the published version available on the publisher's web site. Cite as the published version.

Author Accepted Manuscripts

If this document is identified as the Author Accepted Manuscript it is the version after peer review but before type setting, copy editing or publisher branding. Cite as Surname, Initial. (Year) 'Title of article'. To be published in *Title of Journal*, Volume and issue numbers [peer-reviewed accepted version]. Available at: DOI or URL (Accessed: date).

Enquiries

If you have questions about this document contact ResearchSupport@kent.ac.uk. Please include the URL of the record in KAR. If you believe that your, or a third party's rights have been compromised through this document please see our [Take Down policy](https://www.kent.ac.uk/guides/kar-the-kent-academic-repository#policies) (available from <https://www.kent.ac.uk/guides/kar-the-kent-academic-repository#policies>).

Quantized Hamiltonian Curl Forces and Squeezed Light

P. Strange

School of Physical Sciences, University of Kent, Canterbury, Kent, CT2 7NH, UK

(Dated: July 3, 2018)

In this paper we discuss quantum curl forces. We present both the classical and quantum theory of linear curl forces. The quantum theory is shown to reproduce the classical theory precisely if appropriate combinations of eigenfunctions are chosen. A series of examples are used to illustrate the theory and to demonstrate its limitations. Furthermore we are able to point out an analogy between the quantum theory of curl forces and some of the squeezed light states of quantum optics.

I. INTRODUCTION

In recent years there has been considerable interest in classical curl forces. These are forces that depend on position, but not velocity and whose curl is non-zero[1]. Such forces are non-conservative and cannot be written as the gradient of a potential, but they are also non-dissipative. The classical theory of such forces has been studied in a systematic and detailed way in a series of papers by Berry and Shukla[1–4]. There appears to be considerable controversy about the existence of such forces in the engineering literature[5], but that is not the focus of this paper and their existence in physics is not in doubt. In the absence of the usual relation between force and potential there would normally be no Hamiltonian or Lagrangian formalism which describes curl forces. However they can be discussed within the generalised Hamiltonian theory of Tvetter[6, 7]. There is also a class of curl forces for which the usual Hamiltonian formalism is applicable[3]. These are cases where the Hamiltonian has an anisotropic quadratic dependence on momentum and it is these forces we discuss in this paper. It does not include the most well-known curl force which is the magnetic Lorentz force. There are examples of curl forces in nature, in particular some of the forces exerted by light on small particles and applications in optical tweezers[8]. Another example is the force felt by an electron in a semiconductor with a donor impurity where the band structure and hence the effective mass becomes anisotropic[9]. In recent times an interesting development in the subject has been the application of the theory of curl forces in statistical mechanics[10]

In general it is not at all clear how to treat curl forces quantum mechanically. However for Hamiltonian curl forces there is a straightforward procedure towards a quantum theory and we develop that here as a first step towards a full quantum theory of curl forces. In the following two sections we set up the classical theory of Hamiltonian curl forces and illustrate it with a few simple examples. Then in section IV we write down and derive the equations describing the quantum theory of curl forces. In section V we solve these equations and show that the classical theory is recovered under certain conditions[14, 15]. We then go on to show that the theory also yields some non-classical behaviour which can be viewed as a representation of certain states of squeezed light[19, 20]. Finally we bring together our results and draw some conclusions from the work.

II. CLASSICAL HAMILTONIAN CURL FORCES

Here we summarise the classical theory of linear curl forces. Sections II and III follow the work of Berry and Shukla [3] closely and are included because later we will demonstrate an equivalence between some equations from the classical theory and some from the quantum theory. It is sufficient to work in two dimensions and under very general assumptions the Hamiltonian can be written as

$$H = \frac{1}{2m}\alpha p_x^2 + \frac{1}{m}\beta p_x p_y + \frac{1}{2m}\gamma p_y^2 + U(x, y) \quad (1)$$

The first of Hamilton's equations then give

$$\begin{aligned} \dot{x} &= \alpha \frac{p_x}{m} + \beta \frac{p_y}{m} \\ \dot{y} &= \beta \frac{p_x}{m} + \gamma \frac{p_y}{m} \end{aligned} \quad (2)$$

We can then get the forces from Hamilton's second equations

$$\begin{aligned} F_x = m\ddot{x} &= \alpha \dot{p}_x + \beta \dot{p}_y = -\alpha \frac{\partial U(x, y)}{\partial x} - \beta \frac{\partial U(x, y)}{\partial y} \\ F_y = m\ddot{y} &= \beta \dot{p}_x + \gamma \dot{p}_y = -\beta \frac{\partial U(x, y)}{\partial x} - \gamma \frac{\partial U(x, y)}{\partial y} \end{aligned} \quad (3)$$

The curl is

$$\Omega = \nabla \times \mathbf{F} = (\alpha - \gamma) \frac{\partial^2 U(x, y)}{\partial x \partial y} + \beta \left(\frac{\partial^2 U(x, y)}{\partial y^2} - \frac{\partial^2 U(x, y)}{\partial x^2} \right) \quad (4)$$

III. CLASSICAL LINEAR CURL FORCES

Now we are going to restrict ourselves to considering linear curl forces for which

$$F_x = ax + by \quad F_y = cx + dy \quad (5)$$

Clearly this is reminiscent of the harmonic oscillator. The kinetic energy parameters and the potential are then given by

$$\alpha = \frac{1}{c}, \quad \beta = 0, \quad \gamma = \frac{1}{b} \quad (6)$$

$$U(x, y) = -\frac{1}{2}acx^2 - bcxy - \frac{1}{2}bdy^2 \quad (7)$$

Then

$$\Omega = c - b \quad (8)$$

which shows that this is indeed a curl force provided $b \neq c$. For the forces (5) we can write

$$\mathbf{F} = m\ddot{\mathbf{r}}(t) = q\mathbf{r}(t) \quad (9)$$

with the dynamical matrix

$$q = \begin{pmatrix} a & b \\ c & d \end{pmatrix} \quad (10)$$

and we must have $b \neq c$ for curl forces. The eigenvalues of this matrix are

$$q_{\pm} = \frac{1}{2} \left(a + d \pm \sqrt{4bc + (a - d)^2} \right) \quad (11)$$

For this orbit to exhibit oscillations requires q_{\pm} to be negative and for a periodic orbit we must require

$$M^2 q_+ = N^2 q_- \quad (12)$$

where M and N are coprime integers. After some algebra this tells us that

$$\begin{aligned} q_+ &= N^2 \frac{a + d}{M^2 + N^2} & q_- &= M^2 \frac{a + d}{M^2 + N^2} \\ bc &= \frac{ad(M^4 + N^4) - (a^2 + d^2)M^2 N^2}{(M^2 + N^2)^2} \end{aligned} \quad (13)$$

Without loss of generality we can take $b = 1$ and for oscillations we require $a + d < 0$. Then the elements of the dynamical matrix are

$$\begin{aligned} a &= -A & b &= 1 \\ c &= \frac{AD(M^4 + N^4) - (A^2 + D^2)M^2 N^2}{(M^2 + N^2)^2} & d &= -D \end{aligned} \quad (14)$$

It is also convenient to define

$$\zeta = \sqrt{\frac{A + D}{M^2 + N^2}} \quad (15)$$

It is now straightforward to solve equation (9) (with mathematica) to get

$$\begin{aligned} x(t) &= x(0) \frac{(AM^2 - DN^2) \cos(\zeta Mt) + (DM^2 - AN^2) \cos(\zeta Nt)}{(A + D)(M^2 - N^2)} \\ &+ y(0) \frac{\cos(\zeta Nt) - \cos(\zeta Mt)}{\zeta^2(M^2 - N^2)} \end{aligned}$$

$$\begin{aligned}
& + v_x(0) \frac{(AM^2 - DN^2)N \sin(\zeta Nt) + (DM^2 - AN^2)M \sin(\zeta Nt)}{\zeta(A + D)MN(M^2 - N^2)} \\
& + v_y(0) \frac{M \sin(\zeta Nt) - N \sin(\zeta Mt)}{\zeta^3 MN(M^2 - N^2)}
\end{aligned} \tag{16}$$

$$\begin{aligned}
y(t) & = x(0) \frac{(DM^2 - AN^2)(AM^2 - DN^2)(\cos(\zeta Nt) - \cos(\zeta Mt))}{(A + D)(M^4 - N^4)} \\
& + y(0) \frac{(AM^2 - DN^2) \cos(\zeta Nt) + (DM^2 - AN^2) \cos(\zeta Mt)}{(A + D)(M^2 - N^2)} \\
& + v_x(0) \frac{(DM^2 - AN^2)(AM^2 - DN^2)(M \sin(\zeta Nt) - N \sin(\zeta Mt))}{\zeta(A + D)MN(M^4 - N^4)} \\
& + v_y(0) \frac{(AM^2 - DN^2)M \sin(\zeta Nt) + (DM^2 - AN^2)N \sin(\zeta Mt)}{\zeta(A + D)MN(M^2 - N^2)}
\end{aligned} \tag{17}$$

The expression for $y(t)$ differs slightly from that of Berry and Shukla[3] but does reproduce their diagrams precisely, we believe that this is due to a typo in their paper. To solve the equations of motion for a particular curl force the procedure is to select A , D , M and N . $b = 1$ and c can be calculated from equation (14). Then we choose the initial position $(x(0), y(0))$ and velocity $(v_x(0), v_y(0))$ of the particle and it becomes a straightforward matter to use equations (16) and (17) to determine the position of the particle at future times. Several examples are displayed in Figure 1.

The curl forces we have generated here are only a very small subset of those possible. They are closed in phase space. That means that the kinetic energy is unchanged after each orbit. However Stokes's theorem implies that the change in kinetic energy around each orbit is

$$\frac{1}{2} \oint \frac{d}{ds} (\mathbf{v} \cdot \mathbf{v}) ds = \oint \ddot{\mathbf{r}} \cdot d\mathbf{r} = \oint F(\mathbf{r}) d\mathbf{r} = \int \int \nabla \times \mathbf{F}(\mathbf{r}) dS \tag{18}$$

where s denotes arc-length around the orbit and the final double integral is over any surface spanning the closed orbit. This integral is indeed zero for all the orbits above. In Figure 1a the orbit is self-retracing and so encloses no area. The other figures involve self-crossing periodic orbits which divides them up into areas where the flux crosses the surface in opposite directions and cancels.

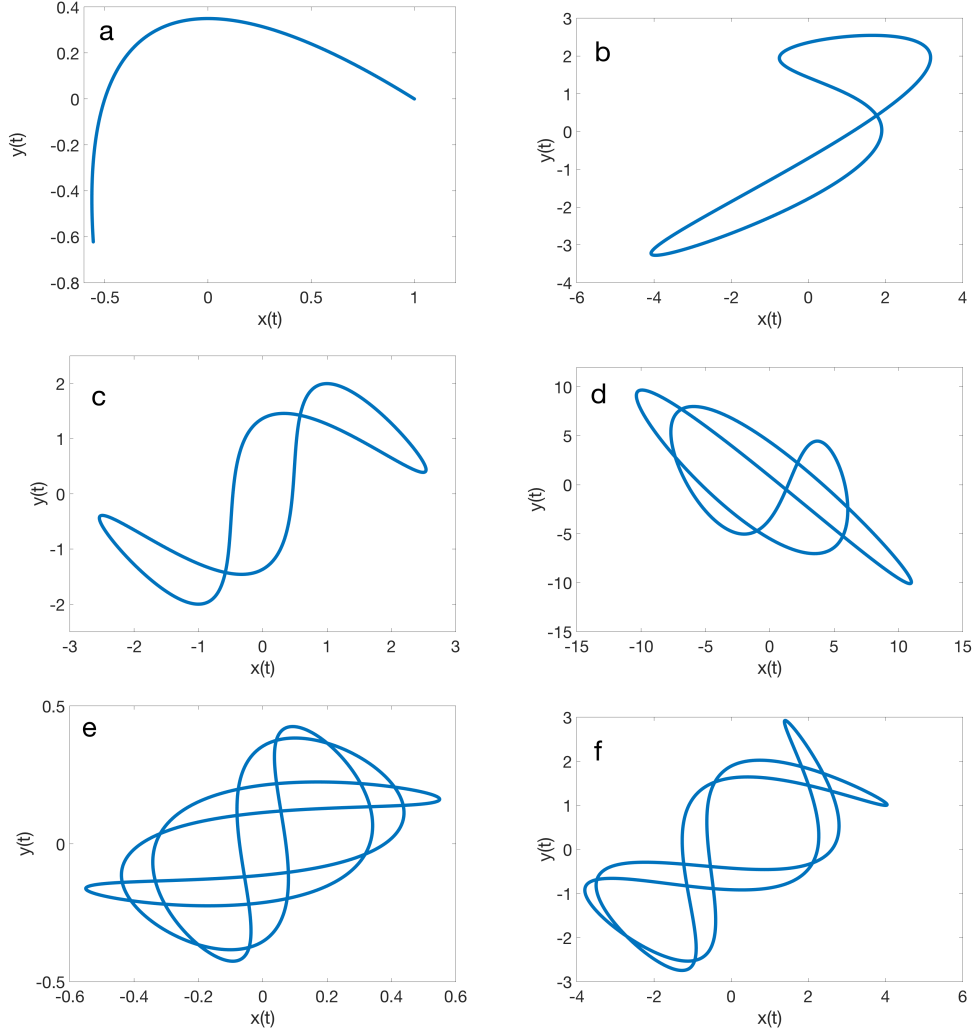


FIG. 1: Figure 1: A selection of periodic orbits generated using equations (??) and (17). These are for values of $(A, D, M, N, x(0), y(0), v_x(0), v_y(0))$ given by: a. $(1, 2, 1, 2, 1, 0, 0, 0)$; b. $(2, 0.2, 1, 2, 1, 1, 2, -1)$; c. $(1, 2, 1, 3, 1, 2, 1, 0)$; d. $(1, 3.5, 3, 2, 3, 4, 3, 4)$; e. $(1.800, 1.461, 3, 5, -0.1, 0.1, 0.6, 0.1)$; f. $(1, 1, 2, 5, 4, 1, 0.5, 0)$.

IV. QUANTUM LINEAR CURL FORCES

Above we have described and made statements about classical Hamiltonian curl forces based on the work of Berry and Shukla[1, 3]. Now we go on to see how to do the equivalent quantum mechanical calculations.

A. The Hamiltonian

The Schrodinger Hamiltonian consistent with the classical theory of section III is

$$\hat{H} = -\frac{\hbar^2\alpha}{2m} \frac{d^2}{dx^2} - \frac{\hbar^2\gamma}{2m} \frac{d^2}{dy^2} + V(\hat{x}, \hat{y}) \quad (19)$$

with

$$V(\hat{x}, \hat{y}) = -\frac{1}{2}ac\hat{x}^2 - bc\hat{x}\hat{y} - \frac{1}{2}bd\hat{y}^2 \quad (20)$$

This is clearly equivalent to a two-body Hamiltonian. To be as consistent as possible with the classical case we choose

$$\alpha = 1/c \quad \gamma = 1/b. \quad (21)$$

This is equivalent to a system where the mass becomes a tensor quantity (This occurs in anisotropic materials where the effective mass of the electrons is dependent on direction in the crystal[9]). We then choose

$$A = -a, \quad D = -d, \quad b = 1 \quad C = c > 0 \quad (22)$$

which means $\gamma = 1$ and the potential becomes

$$V(\hat{x}, \hat{y}) = \frac{1}{2}AC\hat{x}^2 - C\hat{x}\hat{y} + \frac{1}{2}D\hat{y}^2 \quad (23)$$

which is the potential energy associated with two coupled harmonic oscillators. Defining the effective spring constants accordingly as

$$k_1 = C(A - 1), \quad k_2 = D - C, \quad \kappa = C \quad (24)$$

and with $m_1 = cm$ and $m_2 = bm$ we have

$$\hat{H} = -\frac{\hbar^2}{2m_1} \frac{d^2}{dx^2} - \frac{\hbar^2}{2m_2} \frac{d^2}{dy^2} + \frac{1}{2}k_1\hat{x}^2 + \frac{1}{2}k_2\hat{y}^2 - \frac{1}{2}\kappa(\hat{x} - \hat{y})^2 \quad (25)$$

This is the Hamiltonian associated with two coupled oscillators which can be solved using standard methods[13]. Defining

$$\mu = (m_1m_2)^{1/2} \quad \omega_1 = \sqrt{\frac{k_1}{m_1}} \quad \omega_2 = \sqrt{\frac{k_2}{m_2}} \quad (26)$$

eventually leads to

$$\hat{H} = \frac{\hat{p}_{x1}^2}{2\mu} + \frac{\hat{p}_{y1}^2}{2\mu} + \frac{1}{2}\mu\omega_-^2\hat{x}_1^2 + \frac{1}{2}\mu\omega_+^2\hat{y}_1^2 \quad (27)$$

with

$$\begin{aligned}\omega_- &= \left(\omega_1^2 \cos^2 \eta + \omega_2^2 \sin^2 \eta + \frac{\kappa}{\mu} \left(\left(\frac{m_1}{m_2} \right)^{1/4} \sin \eta - \left(\frac{m_2}{m_1} \right)^{1/4} \cos \eta \right)^2 \right)^{1/2} \\ \omega_+ &= \left(\omega_1^2 \sin^2 \eta + \omega_2^2 \cos^2 \eta + \frac{\kappa}{\mu} \left(\left(\frac{m_1}{m_2} \right)^{1/4} \cos \eta + \left(\frac{m_2}{m_1} \right)^{1/4} \sin \eta \right)^2 \right)^{1/2}\end{aligned}\quad (28)$$

and

$$\eta = \frac{1}{2} \arctan \left(\frac{2\kappa/\mu}{\omega_2^2 - \omega_1^2 + \kappa(m_1 - m_2)/\mu^2} \right). \quad (29)$$

Equation (27) is a two-dimensional single particle Simple Harmonic Oscillator hamiltonian with suitably transformed coordinates (x_1, y_1) . If we define a wavefunction

$$\Psi(x_1, y_1, t) = \Phi(x_1, t)\psi(y_1, t) \quad (30)$$

and separate the Schrodinger equation for this Hamiltonian we find

$$\begin{aligned}-\frac{\hbar^2}{2\mu} \frac{d^2\Phi(x_1)}{dx_1^2} + \frac{1}{2}\mu\omega_-^2 x_1^2 \Phi(x_1) &= E_x \Phi(x) \\ -\frac{\hbar^2}{2\mu} \frac{d^2\psi(y_1)}{dy_1^2} + \frac{1}{2}\mu\omega_+^2 y_1^2 \psi(y_1) &= E_y \psi(y)\end{aligned}\quad (31)$$

V. SOLUTIONS

The Schrodinger equations above are solved in most quantum mechanics text books and their general form is straightforwardly written as

$$\Psi_n(z, t) = \left(\frac{1}{2^n n!} \right)^{1/2} \left(\frac{m\omega}{\pi \hbar} \right)^{1/4} H_n \left(\left(\frac{m\omega}{\hbar} \right)^{1/2} z \right) \exp \left(-\frac{m\omega z^2}{2\hbar} \right) \exp(-i(n+1/2)\omega t) \quad (32)$$

where $H_n(z)$ are Hermite polynomials, and we have put back the time dependence. (Ψ here is distinguished from Ψ in equation (30) by the number of arguments in the brackets). Of course, if a single eigenstate is taken as the solution the motion exhibits no overall time dependence and if a linear combination of eigenstates is chosen we get the usual oscillatory time dependence. Throughout the rest of this paper we retain constants in equations, but diagrams are drawn in units in which $\hbar = m = 1$.

There are two operators that commute with the Hamiltonian and hence represent conserved quantities. Firstly there is the hamiltonian itself, simply representing the energy and secondly the operator

$$C_2 = (D - A) \left(\frac{\hat{p}_x^2}{2Cm} - \frac{\hat{p}_y^2}{2Bm} \right) + \frac{2\hat{p}_x \hat{p}_y}{m}$$

$$\frac{1}{2} ((2BC^2 + AC(A - D))\hat{x}^2 - 2BC(A + D)\hat{x}\hat{y} + (2B^2C - BD(A - D))\hat{y}^2) \quad (33)$$

which does not have a clear interpretation and which is analogous to the corresponding classical quantity[3].

A. Coherent States

Of course, any linear combinations of these eigenstates are acceptable solutions of the Schrodinger equations (31). A particularly important example are the Glauber coherent states[12, 14, 15], which, in quantum optics, are known to be a combination of electromagnetic oscillators which reproduce classical light as closely as possible. They accurately describe the quantum state of a laser and have also found application in the description of superfluids[16, 17] and superconductors[18] for example. In the configuration representation they are given by[11, 15]:

$$|\alpha\rangle = e^{-\frac{1}{2}|\alpha|^2} \sum_{n=0}^{\infty} \frac{\alpha^n}{\sqrt{n!}} |n\rangle \quad (34)$$

Here α is a constant (generally complex) which characterises the state and the sum is over time independent harmonic oscillator eigenstates $|n\rangle$. The time dependence evident in equation (32) can be incorporated by replacing α with $\alpha \exp(-i\omega t)$ and including an extra phase factor of $\exp(-i\omega t/2)$ outside the sum.[11, 21]. It is straightforward to calculate the expectation value of position and momentum for these states. For our case:

$$\begin{aligned} \langle \hat{x}_1(t) \rangle &= \sqrt{\frac{2\hbar}{m\omega_-}} |\alpha_x| \cos(\omega_- t - \phi_1) \\ \langle \hat{p}_{x1}(t) \rangle &= -|\alpha_x| \sqrt{2m\hbar\omega_-} \sin(\omega_- t - \phi_1) \end{aligned} \quad (35)$$

and similar expressions can be derived for the y_1 -components. If we translate these back into the original coordinate system we find

$$\begin{aligned} \langle \hat{x}(t) \rangle &= \sqrt{\frac{2\hbar}{m_1}} \left(\frac{|\alpha_x|}{\sqrt{\omega_-}} \cos \eta \cos(\omega_- t - \phi_-) - \frac{|\alpha_y|}{\sqrt{\omega_+}} \sin \eta \cos(\omega_+ t - \phi_+) \right) \\ \langle \hat{y}(t) \rangle &= \sqrt{\frac{2\hbar}{m_2}} \left(\frac{|\alpha_x|}{\sqrt{\omega_-}} \sin \eta \cos(\omega_- t - \phi_-) + \frac{|\alpha_y|}{\sqrt{\omega_+}} \cos \eta \cos(\omega_+ t - \phi_+) \right) \\ \langle \hat{p}_x(t) \rangle &= \sqrt{2\hbar m_1} (-|\alpha_x| \sqrt{\omega_-} \cos \eta \sin(\omega_- t - \phi_-) + |\alpha_y| \sqrt{\omega_+} \sin \eta \sin(\omega_+ t - \phi_+)) \end{aligned}$$

$$\langle \hat{p}_y(t) \rangle = -\sqrt{2\hbar m_2} (|\alpha_x| \sqrt{\omega_-} \sin \eta \sin(\omega_- t - \phi_-) + |\alpha_y| \sqrt{\omega_+} \cos \eta \sin(\omega_+ t - \phi_+)) \quad (36)$$

In these equations α_x , α_y , ϕ_- , and ϕ_+ are unknown. However to remain as close as possible to the classical theory we can find them by specifying $\langle \hat{x}(0) \rangle$, $\langle \hat{y}(0) \rangle$, $\langle \hat{p}_x(0) \rangle$ and $\langle \hat{p}_y(0) \rangle$ as the boundary conditions and rearranging equations (36). This leaves us with four equations and four unknowns:

$$\begin{aligned} \phi_- &= \arctan \left[\frac{1}{m_2 \omega_-} \left(\frac{(m_2)^{1/2} \cos \eta \langle \hat{p}_x(0) \rangle + \sin \eta \langle \hat{p}_y(0) \rangle}{\frac{(m_1)^{1/2} \cos \eta \langle \hat{x}(0) \rangle + \sin \eta \langle \hat{y}(0) \rangle} \right) \right]; \\ \alpha_x &= \frac{1}{\cos \phi_-} \sqrt{\frac{\omega_-}{2\hbar}} \left(m_1^{1/2} \cos \eta \langle \hat{x}(0) \rangle + m_2^{1/2} \sin \eta \langle \hat{y}(0) \rangle \right); \\ \phi_+ &= \arctan \left[\frac{1}{m_1 \omega_+} \left(\frac{\frac{(m_1)^{1/2} \cos \eta \langle \hat{p}_y(0) \rangle - \sin \eta \langle \hat{p}_x(0) \rangle}{\frac{(m_2)^{1/2} \cos \eta \langle \hat{y}(0) \rangle - \sin \eta \langle \hat{x}(0) \rangle} \right) \right]; \\ \alpha_y &= \frac{1}{\cos \phi_+} \sqrt{\frac{\omega_+}{2\hbar}} \left(m_2^{1/2} \cos \eta \langle \hat{y}(0) \rangle - m_1^{1/2} \sin \eta \langle \hat{x}(0) \rangle \right). \end{aligned} \quad (37)$$

With these values of the constants we are now able to apply the quantum theory. We choose values of $\langle \hat{x}(0) \rangle$, $\langle \hat{y}(0) \rangle$, $\langle \hat{v}_x(0) \rangle = \langle \hat{p}_x(0) \rangle / m_1$ and $\langle \hat{v}_y(0) \rangle = \langle \hat{p}_y(0) \rangle / m_2$ in complete analogy with the classical theory. These can be used in equations (37) to evaluate the constants. In turn these can be used in equations (36) to calculate the motion as a function of time in configuration space. To actually determine the particular orbits we also need to choose values of A , B , C and D . As in the classical theory $B = 1$ and we choose A and D . We then have to select C so as to ensure commensurability (a closed orbit). We have found that choosing M and N as in the classical case and using the expression for C generated by equations (14) yields commensurate orbits. Several example orbits have been calculated and these are shown in Figure 2. Here we have chosen identical parameters to some of those shown in Figure 1. Clearly the orbits are identical. This demonstrates unequivocally that our procedure is the right way to treat linear curl forces quantum mechanically. We have not been able to reproduce figures 1b and d using this method. The reason for this is that equation (14) causes C to be negative in these cases. This is allowed in the classical theory. However in quantum mechanics it means that m_1 is negative and ω_1 is imaginary and the resulting Schrodinger equation is no longer equivalent to the harmonic oscillator.

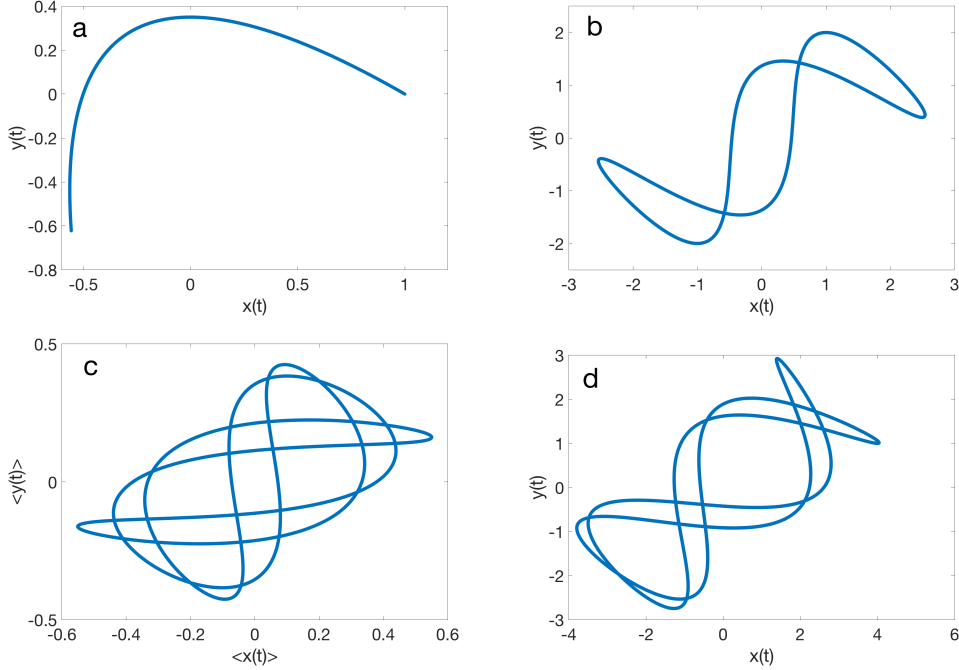


FIG. 2: A selection of periodic orbits calculated as the expectation values $(\langle \hat{x}(t) \rangle, \langle \hat{y}(t) \rangle)$ for the Glauber coherent states. These are for values of $(A, D, M, N, x(0), y(0), v_x(0), v_y(0))$ given by: a. $(1, 2, 1, 2, 1, 0, 0, 0)$; b. $(1, 2, 1, 3, 1, 2, 1, 0)$; c. $(1.800, 1.461, 3, 5, -0.1, 0.1, 0.6, 0.1)$; d. $(1, 1, 2, 5, 4, 1, 0.5, 0)$.

The fact that the orbits in the classical and quantum theory are identical in this case indicates that the theories are mathematically equivalent and indeed this is the case. Equations (36) can be rewritten as coefficients multiplying $\cos \omega_- t$, $\cos \omega_+ t$, $\sin \omega_- t$, and $\sin \omega_+ t$, while equations (16) and (17) can be written as coefficients multiplying $\cos N\zeta t$, $\cos M\zeta t$, $\sin N\zeta t$, and $\sin M\zeta t$. We can then compare coefficients of these quantities and they turn out to be numerically identical. Thus we can relate the parameters in the quantum theory to those on the classical theory. For example from the expressions for $\langle x(t) \rangle$ we find

$$\begin{aligned}
 x(0) \frac{DM^2 - AN^2}{(A+D)(M^2 - N^2)} + y(0) \frac{1}{\zeta^2(M^2 - N^2)} &= \sqrt{\frac{2\hbar}{m_1}} \frac{\alpha_x}{\sqrt{\omega_-}} \cos \eta \cos \phi_- \\
 x(0) \frac{AM^2 - DN^2}{(A+D)(M^2 - N^2)} - y(0) \frac{1}{\zeta^2(M^2 - N^2)} &= -\sqrt{\frac{2\hbar}{m_1}} \frac{\alpha_y}{\sqrt{\omega_+}} \sin \eta \cos \phi_+ \quad (38)
 \end{aligned}$$

and several other similar equations exist. This shows that if the eigenfunctions are the coherent states the motion in configuration space is entirely classical.

We can calculate the expectation values of the square of position and momentum. Then

defining uncertainty in the usual way

$$\Delta A = \sqrt{\langle \hat{A}^2 \rangle - \langle \hat{A} \rangle^2}$$

we get some simple expressions.

$$\begin{aligned} \Delta x &= \sqrt{\frac{\hbar}{2m_1} \left(\frac{\cos^2 \eta}{\omega_-} + \frac{\sin^2 \eta}{\omega_+} \right)^{1/2}} \\ \Delta y &= \sqrt{\frac{\hbar}{2m_2} \left(\frac{\sin^2 \eta}{\omega_-} + \frac{\cos^2 \eta}{\omega_+} \right)^{1/2}} \\ \Delta p_x &= \sqrt{\frac{\hbar m_1}{2} (\omega_- \cos^2 \eta + \omega_+ \sin^2 \eta)^{1/2}} \\ \Delta p_y &= \sqrt{\frac{\hbar m_2}{2} (\omega_- \sin^2 \eta + \omega_+ \cos^2 \eta)^{1/2}} \end{aligned} \quad (39)$$

which are consistent with

$$\Delta x \Delta p_x = \Delta y \Delta p_y \geq \hbar/2 \quad (40)$$

The uncertainties are all time-independent minimum uncertainty states, consistent with what is expected for coherent states.

B. Yurke-Stoler States

Within quantum optics the Glauber coherent states describe light that is as close as possible to our classical notion of light and contains an infinite number of photons. The equivalence between the quantum theory of curl forces described by these coherent states and the classical theory of curl forces leads us to look at other states that are important in quantum optics. It is tempting to examine the odd and even cat-states[11], but their symmetry properties yield $\langle x(t) \rangle = \langle y(t) \rangle = 0$ so no equivalence between classical curl states and the cat states can be found. Therefore we have chosen to consider the Yurke-Stoler states[11, 19, 20] which are defined in terms of the coherent states by

$$|\psi \rangle = \frac{1}{\sqrt{2}} (|\alpha \rangle + i|\alpha \rangle - |\alpha \rangle) \quad (41)$$

In quantum optics these states describe non-classical squeezed light. The squeezing is described by a quadrature operator which is equivalent to the momentum operator for curl forces. If we assume the solutions to equations (31) take this form we can follow a very

similar procedure to the coherent states to determine expressions for the expectation values and they look similar. The coherent states are not orthogonal and obey

$$\langle \alpha | -\alpha \rangle = \exp(-2|\alpha|^2) \quad (42)$$

We find

$$\begin{aligned} \langle \hat{x}(t) \rangle &= \sqrt{\frac{2\hbar}{m_1}} \left(-\frac{|\beta_x|}{\sqrt{\omega_-}} \cos \eta \sin(\omega_- t - \phi_-) - \frac{|\beta_y|}{\sqrt{\omega_+}} \sin \eta \sin(\omega_+ t - \phi_+) \right) \\ \langle \hat{y}(t) \rangle &= -\sqrt{\frac{2\hbar}{m_2}} \left(\frac{\beta_x}{\sqrt{\omega_-}} \sin \eta \sin(\omega_- t - \phi_-) + \frac{|\beta_y|}{\sqrt{\omega_+}} \cos \eta \sin(\omega_+ t - \phi_+) \right) \\ \langle \hat{p}_x(t) \rangle &= \sqrt{2\hbar m_1} (|\beta_x| \sqrt{\omega_-} \cos \eta \cos(\omega_- t - \phi_-) - |\beta_y| \sqrt{\omega_+} \sin \eta \cos(\omega_+ t - \phi_+)) \\ \langle \hat{p}_y(t) \rangle &= -\sqrt{2\hbar m_2} (|\beta_x| \sqrt{\omega_-} \sin \eta \cos(\omega_- t - \phi_-) + |\beta_y| \sqrt{\omega_+} \cos \eta \cos(\omega_+ t - \phi_+)) \end{aligned} \quad (43)$$

where

$$\beta_{x(y)} = \alpha_{x(y)} \exp(-2|\alpha_{x(y)}|^2) \quad (44)$$

The expressions (43) look remarkably similar to equations (36). Comparing the two shows that they are identical apart from $\sin(\omega_{+(-)}t - \phi_{+(-)}) \longleftrightarrow -\cos(\omega_{+(-)}t - \phi_{+(-)})$ and we distinguish the constants β and α between the two cases.

As for the coherent states, the orbits in configuration space for the classical theory and for the quantum theory with the Yurke-Stoler wavefunctions are identical. Some examples of these are shown in Figures 3a and 4a. The expressions for the orbits only differ from those for the coherent states by a phase. So we can go through the same procedure of comparing coefficients of trigonometric functions of time to identify the parameters of the quantum theory with those of the classical theory. For example from the expressions for $\langle x(t) \rangle$ we find the relations equivalent to the expressions 38 are

$$\begin{aligned} x(0) \frac{DM^2 - AN^2}{(A+D)(M^2 - N^2)} + y(0) \frac{1}{\zeta^2(M^2 - N^2)} &= \sqrt{\frac{2\hbar}{m_1}} \frac{\beta_x}{\sqrt{\omega_-}} \cos \eta \sin \phi_- \\ x(0) \frac{AM^2 - DN^2}{(A+D)(M^2 - N^2)} - y(0) \frac{1}{\zeta^2(M^2 - N^2)} &= -\sqrt{\frac{2\hbar}{m_1}} \frac{\beta_y}{\sqrt{\omega_+}} \sin \eta \sin \phi_+ \end{aligned} \quad (45)$$

along with several other similar equations. These differ from the coherent state expressions simply through $\sin \phi_{+(-)} \longleftrightarrow \cos \phi_{+(-)}$. This shows that if the eigenfunctions are the Yurke-Stoler states the motion in configuration space is entirely classical.

Now following a very similar procedure to the coherent states case we can determine the coefficients β_x and β_y . However these coefficients have a maximum value. The function on the right of equation (44) takes on a maximum value of $\exp(-1/2)/2 \approx 0.30326533$ for α real. If either $|\beta_x|$ or $|\beta_y|$ are larger than this there is no Yurke-Stoler state equivalent to that curl force. However if both β_x and β_y are less than this number there are four Yurke-Stoler states equivalent to a single classical curl force. This is because a single value of β in equation (44) yields two possible values of α . It is only β_x, β_y, ϕ_- and ϕ_+ which determine the orbits in configuration and momentum space. However other physically important expectation values depend more directly on $\alpha_{x(y)}$. If we calculate the expectation values of the square of position and momentum we find:

$$\begin{aligned}
\langle \hat{x}^2(t) \rangle &= \frac{2\hbar}{m_1} \left(\frac{\alpha_x^2}{\omega_-} \cos^2 \eta \cos^2(\omega_- t - \phi_-) + \frac{\alpha_y^2}{\omega_+} \sin^2 \eta \cos^2(\omega_+ t - \phi_+) \right. \\
&\quad \left. - 2 \frac{|\beta_x| |\beta_y|}{\sqrt{\omega_- \omega_+}} \sin \eta \cos \eta \sin(\omega_- t - \phi_-) \sin(\omega_+ t - \phi_+) \right) \\
&\quad + \frac{\hbar}{2m_1} \left(\frac{\cos^2 \eta}{\omega_-} + \frac{\sin^2 \eta}{\omega_+} \right); \\
\langle \hat{y}^2(t) \rangle &= \frac{2\hbar}{m_2} \left(\frac{\alpha_x^2}{\omega_-} \sin^2 \eta \cos^2(\omega_- t - \phi_-) + \frac{\alpha_y^2}{\omega_+} \cos^2 \eta \cos^2(\omega_+ t - \phi_+) \right. \\
&\quad \left. + 2 \frac{|\beta_x| |\beta_y|}{\sqrt{\omega_- \omega_+}} \sin \eta \cos \eta \sin(\omega_- t - \phi_-) \sin(\omega_+ t - \phi_+) \right) \\
&\quad + \frac{\hbar}{2m_2} \left(\frac{\sin^2 \eta}{\omega_-} + \frac{\cos^2 \eta}{\omega_+} \right); \\
\langle \hat{p}_x^2(t) \rangle &= 2\hbar m_1 (\alpha_x^2 \omega_- \cos^2 \eta \sin^2(\omega_- t - \phi_-) + \alpha_y^2 \omega_+ \sin^2 \eta \sin^2(\omega_+ t - \phi_+) \\
&\quad - 2|\beta_x| |\beta_y| \sqrt{\omega_- \omega_+} \sin \eta \cos \eta \cos(\omega_- t - \phi_-) \cos(\omega_+ t - \phi_+)) \\
&\quad + \frac{m_1 \hbar}{2} (\omega_- \cos^2 \eta + \omega_+ \sin^2 \eta); \\
\langle \hat{p}_y^2(t) \rangle &= 2\hbar m_2 (\alpha_x^2 \omega_- \sin^2 \eta \sin^2(\omega_- t - \phi_-) + \alpha_y^2 \omega_+ \cos^2 \eta \sin^2(\omega_+ t - \phi_+) \\
&\quad + 2|\beta_x| |\beta_y| \sqrt{\omega_- \omega_+} \sin \eta \cos \eta \cos(\omega_- t - \phi_-) \cos(\omega_+ t - \phi_+)) \\
&\quad + \frac{m_2 \hbar}{2} (\omega_- \sin^2 \eta + \omega_+ \cos^2 \eta); \tag{46}
\end{aligned}$$

which depend on α as well as β .

The structure of these equations is informative. The first two terms and the final term are all real and positive. The final term leads to the minimum uncertainty for the harmonic oscillator which is equal to the uncertainty for the $n = 0$ eigenfunction. However the

third term is real and of indeterminate sign. If it is positive we can, in principle, choose the parameters describing the curl force such that the third term is greater in magnitude than the sum of the first two terms. This will lead to suppression of the $n = 0$ (vacuum) fluctuations and an uncertainty below the usual minimum value. In $\langle \hat{x}^2(t) \rangle$ the third term has the opposite sign to the equivalent term in $\langle \hat{y}^2(t) \rangle$, but is otherwise identical, so any decrease in the uncertainty in $x(t)$ is matched by a corresponding increase in the uncertainty in $y(t)$. Furthermore if we choose the parameters to minimise the position uncertainty the momentum uncertainty will have a tendency to be maximised at the same time because sines and cosines interchange between the two expressions. This mechanism means we are never in danger of breaking the Uncertainty Principle. From equations (43) and (46) we can calculate the uncertainty and in this case it is time-dependent.

In Figure 3. we illustrate the Yurke-Stoler state. For this Hamiltonian we find $\beta_x = 0.1954$ and $\beta_y = 0.2638$. The resulting motion in configuration space is shown in Figure 3a. This orbit is also identical to that found classically and this is generally true provided the coefficients satisfy the above conditions. The values of α_x and α_y consistent with these values of β are $\alpha_x = 0.2141$ or 0.8612 and $\alpha_y = 0.3264$ or 0.6969 . As can be seen in equations (46) the square of the momentum and position depends on α_x and α_y as well as β_x and β_y . so they can take on different values, but are still cyclic. This means that the uncertainty is also cyclic and we plot these as orbits in “uncertainty space” for this case in Figure 3 b-i.

Selecting values of M and N such that $M/N \ll 1$ or $M/N \gg 1$ leads to widely differing values of ω_- and ω_+ . This is what is required to ensure that there are times in the orbit at which the uncertainty goes below the vacuum value. An example is plotted in Figure 4. Here Figures 4a displays the orbit in configuration space. In Figures 4b-i we show the uncertainties again for the different consistent values of α_x and α_y as described in the figure caption. There are several things worthy of note in these figures and in the comparison of them with figure 3. Firstly, Figures 3b-i all appear to be 1-dimensional lines. In fact they are not, but are a continuous curve that periodically crosses itself. However the amplitude of the oscillations is smaller than the width of the line on the diagrams. This is always the same for orbits where we have deliberately chosen the parameters to provide a large difference between ω_- and ω_+ in the examples we have examined. Secondly, the uncertainty figures fall into four pairs, b-d, c-g, e-i and f-h. This does not occur in Figure 3. For example the curves in Figures 4b and d correspond to the same value of α_x and different

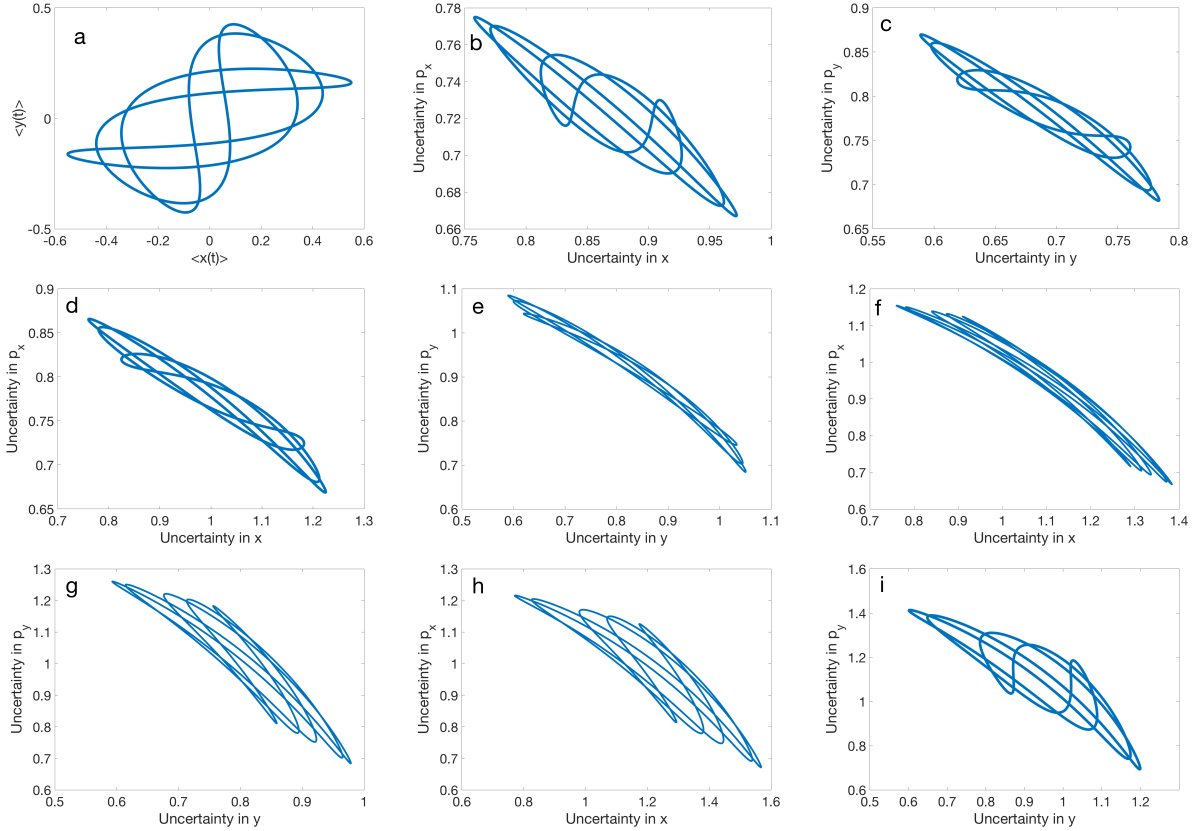


FIG. 3: For the case $(1.8, 1.461, 3, 5, -0.1, 0.1, 0.6, 0.1)$. we find $\beta_x = 0.1954$, $\beta_y = 0.2638$:
a. the particle in orbit in configuration space as described by the expectation values of \hat{x} and \hat{y} ; b. the uncertainties in the x-direction for $\alpha_x = 0.2141$, $\alpha_y = 0.3264$; c. the uncertainties in the y-direction for $\alpha_x = 0.2141$, $\alpha_y = 0.3264$; d. the uncertainties in the x-direction for $\alpha_x = 0.2141$, $\alpha_y = 0.6969$; e. the uncertainties in the y-direction for $\alpha_x = 0.2141$, $\alpha_y = 0.6969$; f. the uncertainties in the x-direction for $\alpha_x = 0.8612$, $\alpha_y = 0.3264$; g. the uncertainties in the y-direction for $\alpha_x = 0.8612$, $\alpha_y = 0.3264$; h. the uncertainties in the x-direction for $\alpha_x = 0.8612$, $\alpha_y = 0.6969$; i. the uncertainties in the x-direction for $\alpha_x = 0.8612$, $\alpha_y = 0.6969$;

α_y . Both the configuration space orbit and the uncertainty in x and p_x are identical, but the uncertainties in y and p_y differ markedly. This works similarly for the other pairs and indicates that the motion in the x and y directions become essentially independent in this limit. Thirdly, in Figure 3. the axes are what we might expect, based on the classical harmonic oscillator. However this is not the case in Figure 4. For the parameters used in Figure 4. we find $\omega_- = 0.9091$ and $\omega_+ = 10.001$. This leads to the vacuum uncertainties

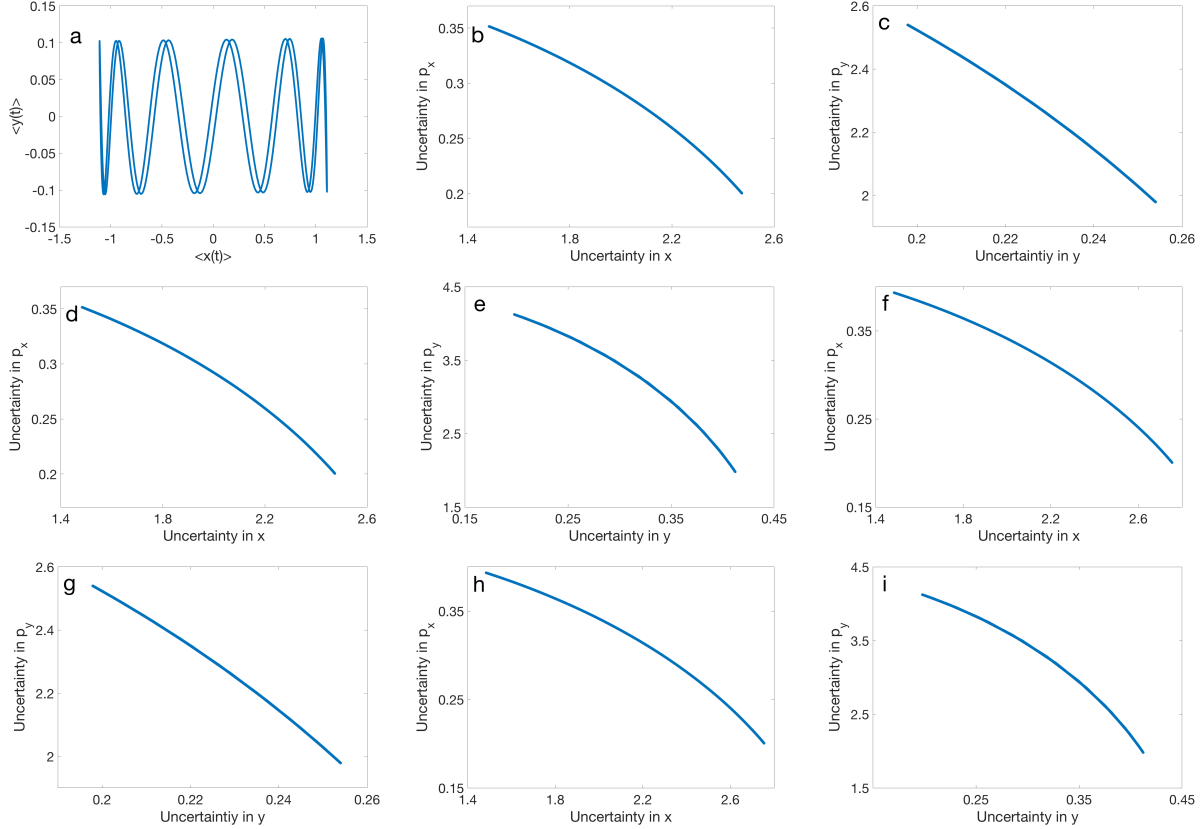


FIG. 4: For the case $(0.82808, 100.0, 11, 1, 0.1, 0.1, 1.0, 0.3)$. we find $\beta_x = 0.2992$, $\beta_y = 0.2330$: a. the particle in orbit in configuration space; b. the uncertainties in the x-direction for $\alpha_x = 0.4428$, $\alpha_y = 0.2694$; c. the uncertainties in the y-direction for $\alpha_x = 0.4428$, $\alpha_y = 0.2694$; d. the uncertainties in the x-direction for $\alpha_x = 0.4428$, $\alpha_y = 0.7747$; e. the uncertainties in the y-direction for $\alpha_x = 0.4428$, $\alpha_y = 0.7747$; f. the uncertainties in the x-direction for $\alpha_x = 0.5595$, $\alpha_y = 0.2694$; g. the uncertainties in the y-direction for $\alpha_x = 0.5595$, $\alpha_y = 0.2694$; h the uncertainties in the x-direction for $\alpha_x = 0.5595$, $\alpha_y = 0.7747$; i. the uncertainties in the y-direction for $\alpha_x = 0.5595$, $\alpha_y = 0.7747$;

$\Delta x = 1.8517$, $\Delta p_x = 0.2700$, $\Delta y = 0.2236$, and $\Delta p_y = 2.2361$. Clearly in Figures 4b, d, f and h the uncertainty in x goes well below this value at the upper end of the curve while at the lower end the uncertainty in p_x is well below the vacuum value. This amounts to about 19% squeezing in position and 25% squeezing in momentum at different points on the orbit. A similar thing happens for the y-components in figures 4c, e, g and i although the squeezing of the y -coordinate in Figure 4 is considerably less than for the other variables

(11% and 10% respectively).

Even in Figure 3 there is some squeezing as the vacuum uncertainties are $\Delta x = 0.8523$, $\Delta p_x = 0.6050$, $\Delta y = 0.6740$, and $\Delta p_y = 0.5156$. This means that there is squeezing of around 10% in the position variables.

VI. CONCLUSIONS

We have considered the class of curl forces most straightforward to quantise, those that can be described within classical Hamiltonian mechanics, and written down the quantum theory to describe them. The Glauber coherent states were used to calculate expectation values of position and momentum and show that they produce paths in configuration space that reproduce those from the classical theory. There is a one-to-one correspondence between the classical and quantum formalisms and we have demonstrated this through several examples. It is interesting to ask whether such forces could be observed. In principle one could set up a two-dimensional anisotropic harmonic trap for cold atoms and observe the orbits through quantum scarring[22–25], although this is likely to be a very challenging experiment.

We have also shown that there is a correspondence between the classical paths and those produced by the quantum mechanical Yurke-Stoler states, but that in this case quantum theory leads to four different states being consistent with the classical theory. These four states lead to identical results for the configuration space orbits, but are distinguished by their expectation values of the square of position and momentum and hence by their uncertainties. For some values of the parameters these are shown to have uncertainties smaller than the vacuum values, in direct analogy with the Yurke-Stoler states of squeezed light. It is clearly possible to reduce the uncertainty in position along one direction and uncertainty in momentum along the perpendicular direction simultaneously. The Yurke-Stoler states are well-known states of squeezed light and there is a one-to-one correspondence between the squeezing of light in these states and the squeezing of the dynamics of particles experiencing curl forces. Thus, one way to think about these curl forces is as a mechanical representation of squeezed light.

This work extends the range of applicability of the coherent states beyond its already broad sphere of application[11, 15–18].

VII. ACKNOWLEDGEMENTS

I would like to thank Rachel Whyman and Johar Ashfaque for some lively and instructive discussions on the topic of curl forces.

-
- [1] M. V. Berry and P. Shukla, *J. Phys. A* **45**, 305201, (2012).
 - [2] M. V. Berry and P. Shukla, *J. Phys. A* **46** 422001, (2013).
 - [3] M. V. Berry and P. Shukla, *Proc. R. Soc. A* **471**, 2015002 (2015).
 - [4] M. V. Berry and P. Shukla, *New. J. Phys* **18** 063018 (2016).
 - [5] I. Eliashkoff, *Appl. Math. Rev.* **58**117, (2005).
 - [6] F. T. Tsveter, *Celestial Mechanics and Dynamical Astronomy*, **60**, issue 4, 409, (1994).
 - [7] F. T. Tsveter, *Journal of Mathematical Physics*, **39**, 1495, (1998).
 - [8] P. Wu, R. Huang, C. Tischer, A. Jonas and E-L Florin, *Phys. Rev. Lett.* **103**, 108101, (2009).
 - [9] M. C. Gutzwiller, *Journal of Mathematical Physics*, **14** 139, (1973).
 - [10] R. S. Wedemann, A. R. Plastino and C. Tsallis, *Phys. Rev. E*, **94**, 062105, (2016).
 - [11] C. Gerry and P. Knight, *Introductory Quantum Optics*, (Cambridge University Press, Cambridge) (2004).
 - [12] S. M. Barnett and P. M. Radmore, *Methods in Theoretical Quantum Optics*, (Oxford Series in Optical and Imaging Science, (Clarendon Press, Oxford), (2002).
 - [13] R. M. McDermott and I. H. Redmount, ArXiv:quant-ph/0403184 (2004).
 - [14] R. J. Glauber, *Phys. Rev. Lett.* **10** 84, (1963).
 - [15] R. J. Glauber, *Phys. Rev* **131**, no 6, 2766, (1963).
 - [16] J. S. Langer, *Phys. Rev.* **167**, 183, (1968).
 - [17] F. W. Cummings and J. R. Johnston, *Phys. Rev.* **151**, 105, (1966).
 - [18] S. Deng, C. Felser and J. Kohler, *Journal of Modern Physics* **4** 10, (2013).
 - [19] B. Yurke and D. Stoler, *Phys. Rev. Lett* **57**, 13, (1986).
 - [20] B. Yurke and D. Stoler, *Phys. Rev. A*, **36**, 1955, (1987).
 - [21] J. J. Sakurai, *Modern Quantum Mechanics*, 2nd Edition, (Addison-Wesley, New York), (1993).
 - [22] T. M. Fromhold, C. R. Tench, S. Bujkiewicz, P. B. Wilkinson and F. W. Sheard, *J. Opt B: Quantum Semiclass. Opt* **26**28, (2000).

- [23] R. G. Scott, S. Bujkiewicz, T. M. Fromhold, P. B. Wilkinson and F. W. Sheard, *Phys. Rev. A* **66**, 023407, (2002).
- [24] J. Larson, B. M. Anderson and A. Altland, *Phys. Rev. A*, **87**, 013624, (2013).
- [25] P. J. J. Luukko, B. Drury, A Klales, L.Kaplan, E. J. Heller, and E. Rasanen, *Sci. Rep.* **6**, 37656, (2016).